3rd IFToMM International Symposium on Robotics and Mechatronics
2 – 4 October 2013, Singapore

BIFURCATION BEHAVIOR OF THE LINE-SYMMETRIC BRICARD LINKAGE WITHOUT OFFSETS

C.-Y. SONG
School of Mechanical and Aerospace Engineering, Nanyang Technological University, Singapore, chaoyangsong@asme.org
Y. CHEN*
Key Laboratory of Mechanism Theory and Equipment Design of Ministry of Education, Tianjin University, China, yan_chen@tju.edu.cn
I.-M. CHEN
School of Mechanical and Aerospace Engineering, Nanyang Technological University, Singapore, michen@ntu.edu.sg

Abstract In this paper, the bifurcation behavior of the line-symmetric Bricard linkages without offset is studied. When there are not offsets, the geometry conditions of the original and revised line-symmetric Bricard linkages become identical to each other. In each linkage, there are two distinct and independent linkage forms. The kinematic paths of each linkage forms in the original and revised linkages are obtained. By inspecting the kinematic paths, certain configurations of these linkage forms are found to be identical to each other, which make it possible for kinematic singularities. As a result, a full map of bifurcation is established for the line-symmetric Bricard linkages without offset, which makes the linkage a good source of design for reconfigurable mechanisms.

Keywords Kinematics, Bricard linkage, multiple closures

Notations

z_i : The coordinate axis along the revolute axis of joints i ;

x_i : The coordinate axis along the common normal between joint axes from joint i to joint $i+1$;

$a_{i(i+1)}$: The length of link $i(i+1)$, which is the common normal distance from z_i to z_{i+1} positively about x_i , and defined in the range of $(-\infty, +\infty)$;

$\alpha_{i(i+1)}$: The twist of link $i(i+1)$, which is the rotation angle from z_i to z_{i+1} positively about x_i , and defined in the range of $[-\pi, \pi)$;

R_i : The offset of joint i , which is the common normal distance from x_i to x_{i+1} positively along z_i , and defined in the range of $(-\infty, +\infty)$;

θ_i : The revolute variable of joint i , which is the rotation angle from x_i to x_{i+1} positively about z_i , and defined in the range of $[-\pi, \pi)$;

Aterm , *Bterm* and *Cterm* : The symbols of simplified mathematical relationships;

a/α , b/β , c/γ , d/δ : the length and twist of the link, e.g. a/α is a link with length a and twist α ;

and Form I, II: The different linkage closures.

X and X′: X is for the parameters in the *original* general line-symmetric Bricard linkage and X′ is for the corresponding parameters in the *revised* linkage.

1. INTRODUCTION

The overconstrained linkage is a kind of mechanism that preserves mobility during a full-circle movement while does not comply with the Grübler-Kutzbach's mobility criterion [1]. The Bricard linkages are an important linkage family in the overconstrained linkages with revolute joints only. The line-symmetric Bricard linkage is one of the Bricard linkages [2, 3] which exhibit line-symmetry in geometry conditions and has only one degree-of-freedom in 3D space. There are two types of the general line-symmetric Bricard linkages reported in literatures. The original linkage was proposed by Bricard [3] as an extension of his work in finding deformable mechanisms with solid angles and dihedrals. This original linkage is line-symmetric in geometry conditions, kinematic variables and spatial configurations [4]. The revised linkage was reported by Mavroidis and Roth [5] when they were searching for new and revised overconstrained linkages using numerical method. This revised linkage differs from the original one with negatively equalled offsets on the opposite joints. The D-H parameters [6] in Figure 1 are adopted in this paper. Therefore, the geometry conditions of the *original* and *revised* general line-symmetric Bricard linkage are

$$\begin{aligned} &a_{i(i+1)} = a'_{i(i+1)} = a_{(i+3)(i+4)} = a'_{(i+3)(i+4)}, \\ &\alpha_{i(i+1)} = \alpha'_{i(i+1)} = \alpha_{(i+3)(i+4)} = \alpha'_{(i+3)(i+4)}, \\ &R_i = R'_i = R_{(i+3)} = -R'_{(i+3)} \quad (i = 1, 2, 3). \end{aligned} \tag{1}$$

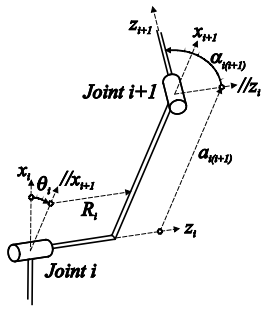

Figure 1 The setup of the Denavit and Hartenberg's parameters.

Note that to ensure this is a closed-loop 6*R* mechanism, the subscripts must be the remainder of 6 in positive numbers. The positively equalled offsets on the opposite joints $R_i = R_{(i+3)}$ correspond to the original linkage [3], while the negatively equalled offsets on the opposite joints $R'_i = -R'_{(i+3)}$ correspond to the revised linkage [5]. It is discussed in [7] that the revised linkage is equivalent to the original linkage with different setups on the joints axis directions. When there's no offset in Eq. (1), the geometry conditions of these two linkages become identical to each other, which is a very special case of the general line-symmetric Bricard linkage.

The focus of this paper is to study the relationship between the original and revised line-symmetric Bricard linkage without offset. Fundamental research into such special cases explores potential designs of reconfiguration mechanisms using kinematic singularities. The layout of this paper is as follows. Section 2 introduces the kinematics of the original and revised line-symmetric Bricard linkage without offsets. Section 3 investigates the bifurcation behaviour of the line-symmetric Bricard linkage without offsets. Conclusion and discussions are made in section 4, which concludes this paper.

2. THE LINE-SYMMETRIC BRICARD LINKAGE WITHOUT OFFSETS

The explicit closure equations of the *original* and *revised* general line-symmetric Bricard linkage are already derived in [7]. We can directly substitute the condition $R_i = 0$ to obtain the explicit closure equations of the original line-symmetric Bricard linkage without offsets. For original Form I linkage, we have

$$\begin{cases} \theta_2 = 2\tan^{-1}\left(\dfrac{-Bterm_2 + \sqrt{Bterm_2^2 - 4Aterm_2 \cdot Cterm_2}}{2Aterm_2}\right) \\ \theta_3 = 2\tan^{-1}\left(\dfrac{-Bterm_3 - \sqrt{Bterm_3^2 - 4Aterm_3 \cdot Cterm_3}}{2Aterm_3}\right) \\ \theta_4 = \theta_1 \\ \theta_5 = \theta_2 \\ \theta_6 = \theta_3 \end{cases}, \tag{2}$$

and for original Form II linkage, we have

$$\begin{cases} \theta_2 = 2\tan^{-1}\left(\dfrac{-Bterm_2 - \sqrt{Bterm_2^2 - 4Aterm_2 \cdot Cterm_2}}{2Aterm_2}\right) \\ \theta_3 = 2\tan^{-1}\left(\dfrac{-Bterm_3 + \sqrt{Bterm_3^2 - 4Aterm_3 \cdot Cterm_3}}{2Aterm_3}\right) \\ \theta_4 = \theta_1 \\ \theta_5 = \theta_2 \\ \theta_6 = \theta_3 \end{cases}. \tag{3}$$

The unknown symbols are defined as follows.

$$\begin{cases} Aterm_2 = \left[a_{34}\sin(\alpha_{12} - \alpha_{23}) + (a_{12} - a_{23})\sin\alpha_{34}\right]\sin\theta_1 \\ Bterm_2 = 2\left[(a_{23}\sin\alpha_{12}\cos\alpha_{34} + a_{12}\sin\alpha_{23}) + (a_{23}\cos\alpha_{12}\sin\alpha_{34} + a_{34}\sin\alpha_{23})\cos\theta_1\right] \\ Cterm_2 = \left[a_{34}\sin(\alpha_{12} + \alpha_{23}) + (a_{12} + a_{23})\sin\alpha_{34}\right]\sin\theta_1 , \end{cases} \tag{4}$$

and

$$\begin{cases} Aterm_3 = \left[a_{12}\sin(\alpha_{34} - \alpha_{23}) + (a_{34} - a_{23})\sin\alpha_{12}\right]\sin\theta_1 \\ Bterm_3 = 2\left[(a_{23}\cos\alpha_{12}\sin\alpha_{34} + a_{34}\sin\alpha_{23}) + (a_{23}\sin\alpha_{12}\cos\alpha_{34} + a_{12}\sin\alpha_{23})\cos\theta_1\right] \\ Cterm_3 = \left[a_{12}\sin(\alpha_{34} + \alpha_{23}) + (a_{34} + a_{23})\sin\alpha_{12}\right]\sin\theta_1 . \end{cases} \tag{5}$$

Using the geometry conditions as below, we can plot the kinematic paths and spatial configurations of these two original linkage forms in Figures 2~5.

$$a_{12} = a_{45} = 0.40,\ a_{23} = a_{56} = 0.55,\ a_{34} = a_{61} = 0.72\,; \tag{6}$$

$$\alpha_{12} = \alpha_{45} = 20\pi/180,\ \alpha_{23} = \alpha_{56} = 70\pi/180,\ \alpha_{34} = \alpha_{61} = 120\pi/180\ ;$$
$$R_1 = R_2 = R_3 = R_4 = R_5 = R_6 = 0\ .$$

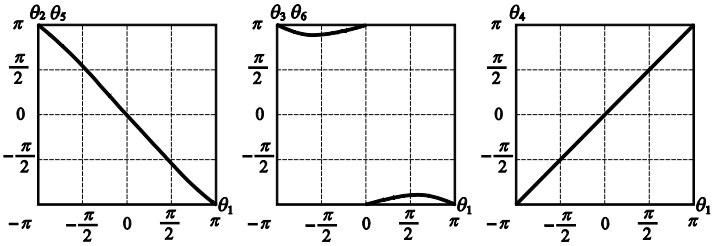

Figure 2 The kinematic paths of the Form I original line-symmetric Bricard linkage with no offsets.

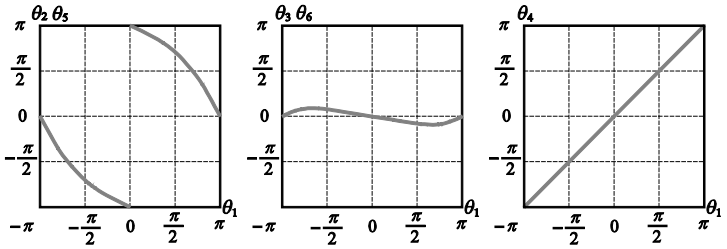

Figure 3 The kinematic paths of the Form II original line-symmetric Bricard linkage with no offsets.

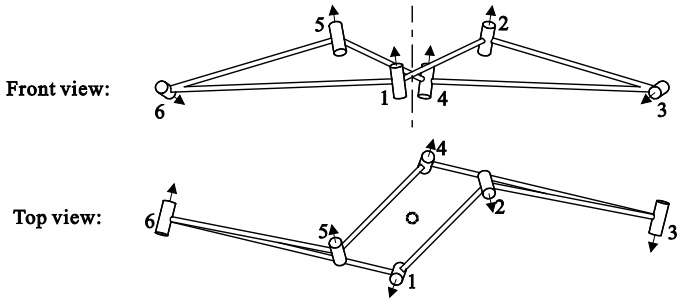

Figure 4 The spatial configuration of the Form I original line-symmetric Bricard linkage with no offsets when $\theta_1^{\mathrm{I}} = \pi/3$.

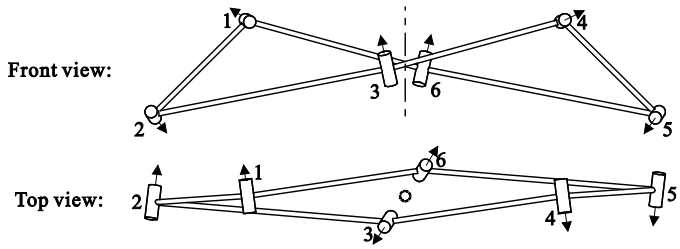

Figure 5 The spatial configuration of the Form II original line-symmetric Bricard linkage with no offsets when $\theta_1^{\mathrm{II}} = \pi/3$.

The revised linkage is equivalent to the original linkage with different setups on the joint axis directions [7]. For example, we can obtain two *revised* linkage forms with the same spatial configurations in Figures 4 and 5 by changing $\alpha_{34} = \alpha_{61} = 120\pi/180$ in Eq. (6) into $\alpha'_{34} = \alpha'_{61} = (120-180)\pi/180 = -60\pi/180$. As a result, the relationship between revolute variables in the *original* and *revised* linkage forms become

$$\theta_1 = \theta'_1,\ \theta_2 = \theta'_2,\ \theta_3 = \theta'_3,\ \theta_4 = -\theta'_4,\ \theta_5 = -\theta'_5,\ \theta_6 = -\theta'_6. \tag{7}$$

3. BIFURCATION ANALYSIS OF THE LINE-SYMMETRIC BRICARD LINKAGE WITHOUT OFFSETS

In the foregoing section, the differentiation between the original and revised linkage forms is based on the *same* spatial configurations between these two linkages under *different* geometry conditions. When all offsets are set to zeros in the general line-symmetric Bricard linkage, the simplified geometry conditions for the *original* and *revised* linkage are the same as follows.

$$a_{i(i+1)} = a_{(i+3)(i+4)},\ \alpha_{i(i+1)} = \alpha_{(i+3)(i+4)},\ R_i = 0\ (i = 1, 2, ..., 6). \tag{8}$$

It would be interesting to study the relationship between the *different* configurations of the original and revised linkages based on the *same* geometry conditions, i.e. Eq. (8). In this case, the original and revised linkages share the *same* geometry conditions, but present with *different* spatial configurations in the 3D space. Using the geometry conditions in Eq. (6), we can also plot the kinematic paths and spatial configurations about the two forms of the revised line-symmetric Bricard linkage in Figures 5~8.

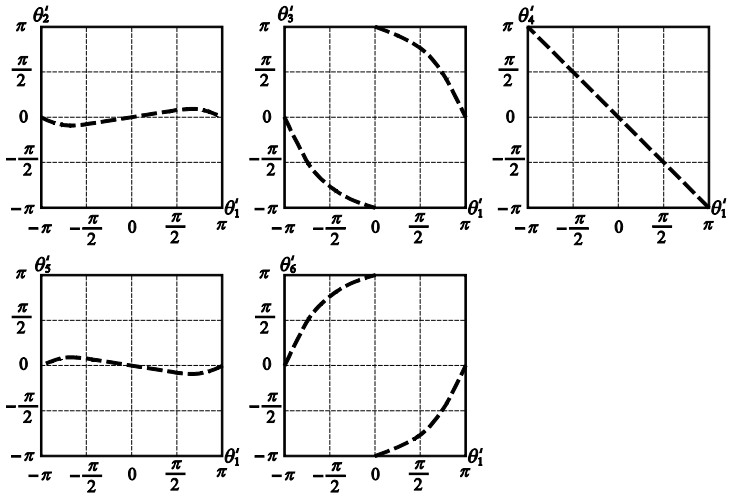

Figure 6 The kinematic paths of the revised Form I′ line-symmetric Bricard linkage with no offsets.

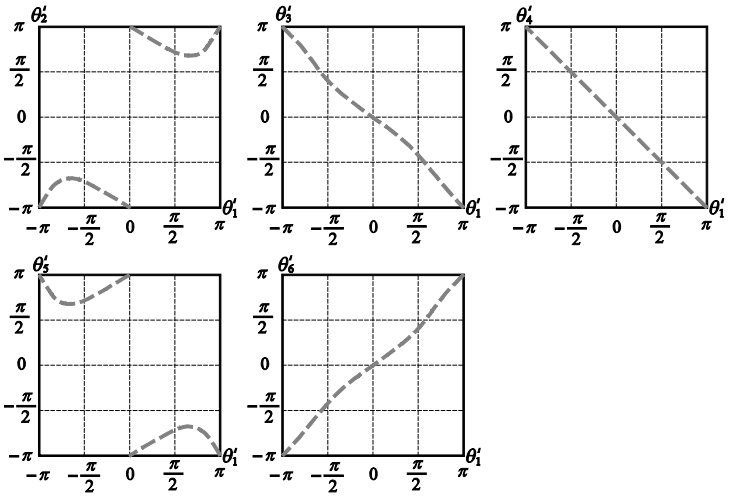

Figure 7 The kinematic paths of the revised Form II′ line-symmetric Bricard linkage with no offsets.

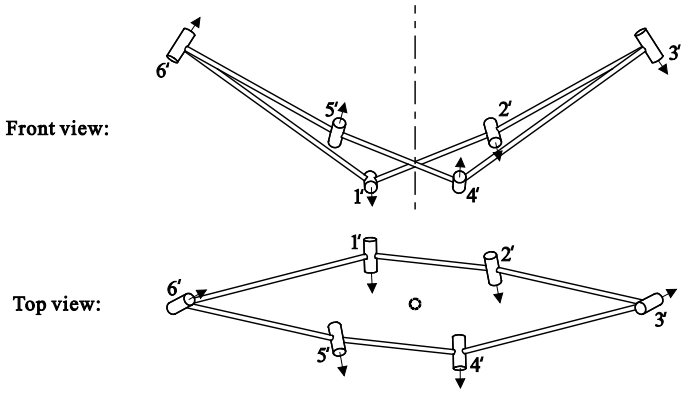

Figure 8 The spatial configuration of the revised Form I′ line-symmetric Bricard linkage with no offsets when $\theta_1^{\mathrm{I}'} = \pi/3$.

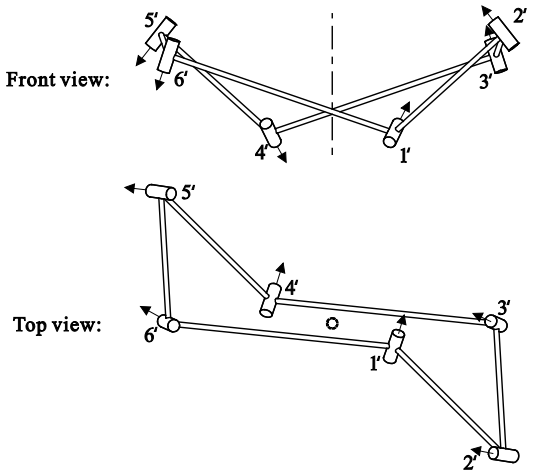

Figure 9 The spatial configuration of the revised Form II′ line-symmetric Bricard linkage with no offsets when $\theta_1^{\mathrm{II}'} = \pi/3$.

By inspecting the kinematic paths of the two original linkage forms in Figures 2 and 3, and that of the two revised linkage forms in Figures 6 and 7, we found certain configurations where the original and revised linkage forms become identical to each other. Take the relationship between θ_1 and θ_5 for example, we can plot the map of transformation in Figure 10, where the kinematic paths of each linkage form is illustrated with the same line types in Figures 2, 3, 6 and 7.

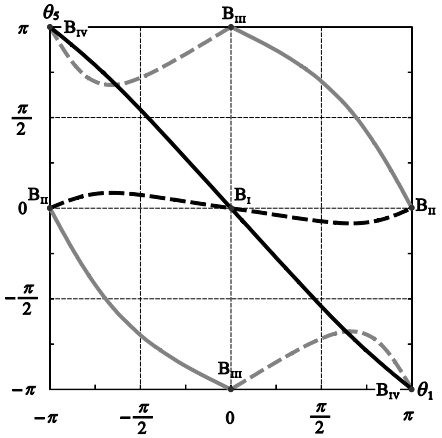

Figure 10 The full map of transformation of the line-symmetric Bricard linkage without offsets.

As shown in Figure 10, when the original Form I linkage in black solid line moves to $\theta_1 = 0$ at $\mathrm{B_I}$, it can bifurcate into the kinematic paths of revised Form I′ linkage in black dash line. Then, when the revised Form I′ linkage in black dash line moves to $\theta_1 = \pi$ at $\mathrm{B_{II}}$, it can bifurcate into the kinematic paths of original Form II linkage in grey solid lines. When the original Form II

linkage in grey solid lines moves to $\theta_1 = 0$ at B_{III}, it can bifurcate into the kinematic paths of revised Form II′ linkage in grey dash lines. Finally, when the revised Form II′ linkage in grey dash lines moves to $\theta_1 = -\pi$ at B_{IV}, it can bifurcate back to the kinematic paths of original Form I linkage in black solid lines. As a result, a full map of bifurcation among these four linkage forms with the identical geometry conditions is obtained. As illustrated in Figure 10, one can conveniently choose other paths for different bifurcation behaviours among these four linkage forms. It should be noticed that here the geometry conditions of the *revised* line-symmetric Bricard linkage without offsets in Eq. (6) is equivalent to the *original* line-symmetric Bricard linkage without offsets under the following geometry conditions, where the twist on links 34 and 61 is changed from $120\pi/180$ to $(120-180)\pi/180 = -60\pi/180$.

$$\begin{gathered} a_{12} = a_{45} = 0.40,\ a_{23} = a_{56} = 0.55,\ a_{34} = a_{61} = 0.72\ ; \\ \alpha_{12} = \alpha_{45} = 20\pi/180,\ \alpha_{23} = \alpha_{56} = 70\pi/180,\ \alpha_{34} = \alpha_{61} = -60\pi/180\ ; \\ R_i = 0\ (i = 1, 2, ..., 6)\,. \end{gathered} \tag{9}$$

Therefore, the full map of transformation in Figure 10 could be alternatively viewed as the transformation among the two forms of *original* line-symmetric Bricard linkage with Eq. (6) in black lines, and two forms of *original* line-symmetric Bricard linkage with Eq. (9) in grey lines.

The above result is verified using the Singular Value Decomposition (SVD) method [8, 9]. The SVD method is to solve the linkage's Jacobian matrix with a predictor and corrector step. Six singular values of the linkage's Jacobian matrix are monitored. When the sixth singular value remains zero, it indicates that the linkage has only one degree of freedom. When the fifth singular value falls to zero at some points, it indicates that the instantaneous mobility is increased in at these points. These points are the bifurcation points where the linkage might bifurcate into other kinematic paths. The SVD results of the original and revised line-symmetric Bricard linkages without offsets are plotted in Figures 11 and 12. Bifurcations of the original and revised linkage forms occur at $\theta_1 = -\pi, 0, +\pi$, which corresponds to the bifurcation behaviours shown in Figure 10.

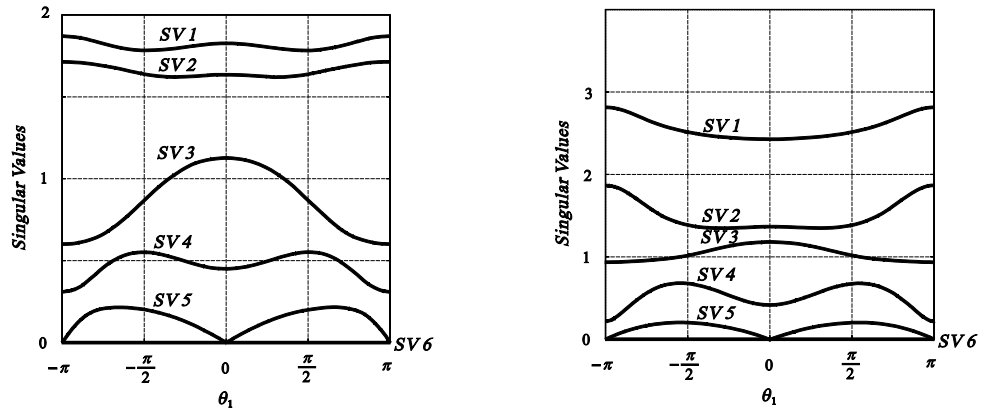

Figure 11 The SVD result of the original line-symmetric Bricard linkage without offsets: (a) the Form I linkage; (b) the Form II linkage.

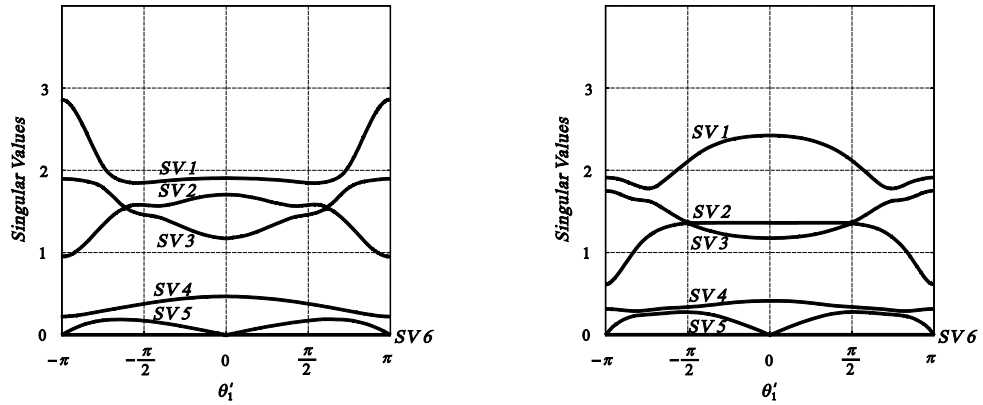

Figure 12 The SVD result of the revised line-symmetric Bricard linkage without offsets: (a) the Form I′ linkage; (b) the Form II′ linkage.

4. CONCLUSION AND DISCUSSIONS

In this paper, the kinematics is devoted to the bifurcation analysis of the line-symmetric Bricard linkage without offsets. It is already discussed that there are two distinct and independent linkage forms in the original and revised general line-symmetric Bricard linkages, respectively. And the original and revised linkages are equivalent to each other with different setups on the joint axes, which result in different representations of the offsets [7]. However, when there are no offsets, the geometry conditions of the original and revised linkages become identical to each other. This change in the geometry conditions makes it possible to connect the kinematic paths of these two linkages through kinematic singularities. As a result, certain points on the kinematic paths are identified where the spatial configurations of the original and revised linkages become identical. At these points, bifurcations may occur and therefore a full map of transformation among different forms of the line-symmetric Bricard linkage without offsets is established.

Such bifurcation behavior makes the line-symmetric Bricard linkage without offsets a good source of design for reconfigurable mechanisms. For example, it could be used to explain to multiple linkage forms and bifurcation behaviors of the double-subtractive-Goldberg 6*R* linkage [10].As shown in Figure 13, the geometry conditions of the double-subtractive Goldberg 6*R* linkage is as follows. We could introduce a new link-pair 56'-6'1 to form a Bennett linkage with link-pair 56-61 and then remove link-pair 56-61 to obtain a line-symmetric Bricard linkage without offset [11]. Therefore, the double-subtractive-Goldberg 6*R* linkage and the line-symmetric Bricard linkage without offsets should share the same bifurcation behaviors.

$$\begin{gathered} a_{12} = a_{45} = a - c\,,\ a_{23} = a_{61} = d\,,\ a_{34} = a_{56} = b\,, \\ \alpha_{12} = \alpha_{45} = \alpha - \gamma\,,\ \alpha_{23} = \alpha_{61} = \delta\,,\ \alpha_{34} = \alpha_{56} = \beta\,, \\ \frac{\sin\alpha}{a} = \frac{\sin\beta}{b} = \frac{\sin\gamma}{c} = \frac{\sin\delta}{d}\,, \\ R_i = 0\ (i = 1, 2, ..., 6)\,. \end{gathered} \tag{10}$$

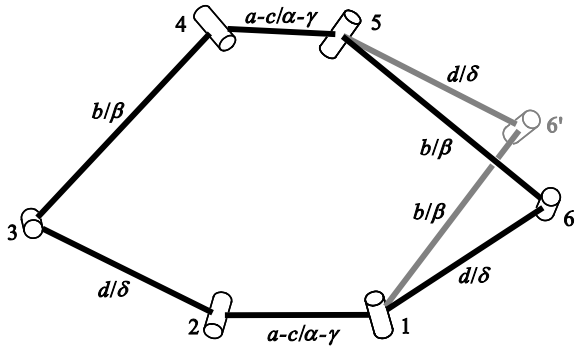

Figure 13 Isomerization on the double-subtractive-Goldberg 6*R* linkage.

Acknowledgments

C.-Y. Song would like to thank NTU for providing the University Graduate Scholarship during his PhD study. Y. Chen would like to thank the financial support from the Natural Science Foundation of China (Projects No. 51275334 and No. 51290293).

REFERENCES

[1] Hunt, K. H., 1990, *Kinematic Geometry of Mechanisms*, Oxford University Press, Oxford.
[2] Bricard, R., 1897, "Mémoire Sur La Théorie De L'octaèdre Articulé," Journal of Pure and Applied Mathematics, 3, pp. 113-150.
[3] Bricard, R., 1927, *Leçons De Cinématique, Tome Ii: Cinématique Appliquée*, Gauthier-Villars, Paris.
[4] Baker, J. E., 1980, "An Analysis of the Bricard Linkages," Mechanism and Machine Theory, 15 (4), pp. 267-286.
[5] Mavroidis, C., and Roth, B., 1995, "New and Revised Overconstrained Mechanisms," Transactions of the ASME: Journal of Mechanical Design, 117 (1), pp. 75.
[6] Denavit, J., and Hartenberg, R. S., 1955, "A Kinematic Notation for Lower-Pair Mechanisms Based on Matrices," Transactions of the ASME: Journal of Applied Mechanics, 23 (1), pp. 215-221.
[7] Song, C. Y., Chen, Y., and Chen, I. M., 2013, "Kinematic Study of the Original and Revised General Line-Symmetric Bricard 6*r* Linkage," pp. (submitted).
[8] Gan, W. W., and Pellegrino, S., 2006, "A Numerical Approach to the Kinematic Analysis of Deployable Structures Forming a Closed Loop," Proceedings of the Institution of Mechanical Engineers, Part C: Journal of Mechanical Engineering Science, 220 (7), pp. 1045-1056.
[9] Pellegrino, S., 1993, "Structural Computations with the Singular Value Decomposition of the Equilibrium Matrix," International Journal of Solids and Structures, 30 (21), pp. 3025-3035.
[10] Song, C. Y., and Chen, Y., 2012, "Multiple Linkage Forms and Bifurcation Behaviours of the Double-Subtractive-Goldberg Linkage," Mechanism and Machine Theory, 57, pp. 95-110.
[11] Wohlhart, K., 1991, "On Isomeric Overconstrained Space Mechanisms," eds., Prague, Czechoslovakia, pp. 153-158.